On the equivalence of OSDM and OTFS

Werf, I. van der; Dol, H. S.; Blom, K. C. H.; Heusdens, R.; Hendriks, R. C.; Leus, G. J. T.

Important note
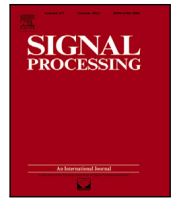To cite this publication, please use the final published version (if applicable).
Please check the document version above.

Short communication

On the equivalence of OSDM and OTFS

Ids van der Werf [a],[*], Henry Dol [b], Koen Blom [b], Richard Heusdens [a],[c], Richard C. Hendriks [a], Geert Leus [a]

[a] *Delft University of Technology, Mekelweg 4, 2628 CD, Delft, The Netherlands*
[b] *TNO, Oude Waalsdorperweg 63, 2597 AK Den Haag, The Netherlands*
[c] *Netherlands Defence Academy (NLDA), Het Nieuwe Diep 8, 1781 AC Den Helder, The Netherlands*

ARTICLE INFO

ABSTRACT

In this paper, we show the mathematical equivalence of two popular modulation schemes: OSDM and OTFS. The former is mainly used in underwater acoustic communications, while the latter scheme is a promising modulation technique in radio-frequency communications. Although literature suggests a link between the two modulation schemes by connecting them to related modulation schemes like V-OFDM and A-OFDM, to the best of the authors' knowledge, a direct mathematical comparison between the schemes has not been presented yet. The main purpose of this paper is therefore to show the mathematical equivalence of the two schemes. In addition, by combining the knowledge of acoustic and radio-frequency communications, we give insight in the performance of OSDM/OTFS in terms of intersymbol interference (ISI) and intercarrier interference (ICI) by analyzing its signal structure.

1. Introduction

The use of mobile communication systems is increasing rapidly. However, as every communication link has certain limitations, more efficient use of existing links is of paramount importance. Modulation is one of the tools that can be used to get the most out of a communication link.

We identify two main fields of research where the design of modulation techniques is addressed: underwater acoustic communications and radio-frequency (RF) communications. In RF communications, high-mobility scenarios and higher/broader frequency bands bring new challenges, including significant delay and Doppler spread due to the frequency selective fading and the dynamics in the environment respectively. Due to the fast attenuation of electromagnetic waves in (sea) water, underwater communication is primarily based on the use of acoustic pressure waves. However, the underwater acoustic channel is often deteriorated by significant delay and Doppler spread as the environmental variability is overlapping with the temporal and spatial scales of the acoustic signals. Causes of variability typically are variations in the sound speed profile, the movement of surface waves and the relative movement of transmitter and receiver.

Although the two fields differ in some aspects, the problems and proposed solutions in terms of modulation techniques are very similar. OSDM and OTFS are two modulation schemes that are used in underwater acoustic communication and radio-frequency communication,

respectively. OTFS involves initially mapping symbols from the delay-Doppler domain to the time–frequency domain and subsequently to the time domain using the Heisenberg transform. OSDM utilizes shift orthogonal sequences and connects OFDM and single carrier (SC) modulation, essentially acting as a precoded variant of OFDM. Due to their distinct origins, the relationship between OTFS and OSDM is not readily apparent. In this paper, we show that OSDM and OTFS are mathematically equivalent, by deriving equivalent input–output relations of both techniques from first principles presented in [1] and [2], respectively.

Throughout this work, the following notation is used. $\mathbf{A}$, $[\mathbf{A}]_{m,n}$ and $\mathbf{a}$ denote a matrix, its element in the m'th row and n'th column, and a vector, respectively. $\mathbf{I}_N$ is the $N \times N$ identity matrix and $\mathbf{1}_{M \times N}$ is the $M \times N$ all ones matrix. $(\cdot)^T$, $(\cdot)^*$ and $(\cdot)^H$ denote the transpose, complex conjugate and Hermitian, respectively. j is used for the imaginary unit, and $\otimes$, $\circ$ and $\odot$ are used for the Kronecker product, Khatri–Rao product (column-wise Kronecker product) and Hadamard product. $\mathbf{F}_N^H$ is the $N \times N$ normalized IDFT matrix with elements $W_N^k = \frac{1}{\sqrt{N}} e^{2\pi j \frac{k}{N}}$.

2. Related work

In RF communication, the conventional modulation technique OFDM, orthogonal frequency-division multiplexing, is not suitable for environments with large Doppler spread, as it will suffer from

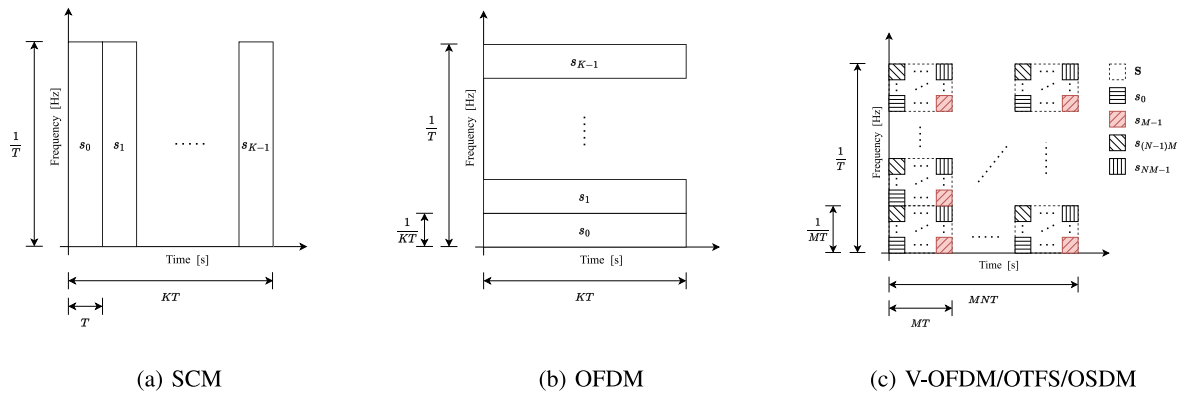(a) SCM   (b) OFDM   (c) V-OFDM/OTFS/OSDM

Fig. 1. Structure of transmitted signal for SCM, OFDM and V-OFDM/OTFS/OSDM.

intercarrier interference (ICI) [3]. Orthogonal time frequency space (OTFS) modulation [2] has therefore become the new state-of-the-art modulation technique being more robust in channels with large Doppler spread.

OTFS modulation defines symbols in the delay-Doppler (DD) domain, after which they are transformed to a time domain signal before transmission. By defining symbols in the DD domain, full channel diversity over time and frequency can be obtained. In general, OTFS is said to be favorable (lower peak-to-average-power ratio (PAPR) and less ICI) in systems with high Doppler and short symbol periods, compared to OFDM [2,4,5]. For that reason, the use of OTFS in 5G networks is currently studied [6,7], and it is considered as one of the contending modulation schemes for 6G networks [8]. Before its first introduction in [2], the OTFS method was patented in the United States by Hadani and Rakib [9].

Generalized frequency division multiplexing (GFDM) [10] was introduced to exploit white spaces in case of (strong) spectrum fragmentation. Compared to OFDM, GFDM has lower PAPR. Nimr et al. [11] extended the GFDM framework and noted that there is a close relationship between GFDM and OTFS. To be more specific, the modulated symbols of GFDM and OTFS are equal up to a permutation.

Asymmetric OFDM (A-OFDM) was proposed to bridge single carrier modulation (SCM) and OFDM, arguing that flexibility between the two increases the overall performance [12]. A-OFDM is based on the divide-and-conquer algorithm, used for the fast Fourier transform (FFT) algorithm. Raviteja et al. [13] showed that A-OFDM is equivalent to OTFS.

In coherent underwater communications, initially, modulation techniques such as SCM [14] and OFDM [15] were used. However, two decades ago, orthogonal signal division multiplexing (OSDM) was introduced as an alternative, which performs much better in terms of bit error rate (BER) and has a lower PAPR [1,16–19].

Xia [20] proposed vector-OFDM (V-OFDM) as a special case of precoded OFDM. Compared to conventional OFDM, the overhead due to the cyclic prefix (CP) is reduced by the use of precoding. In [21,22] the "compatibility" between V-OFDM and OSDM was noted. In [23], the mathematical equivalence between V-OFDM and A-OFDM was remarked. Although the two are equivalent, A-OFDM and V-OFDM seem to be inspired on different principles. Recently, Xia argued that the transmitted signals of V-OFDM and OTFS are the same [24].

As the literature suggests, OSDM and OTFS are related by connecting them with V-OFDM. However, to the best of the authors' knowledge, a direct mathematical comparison is still missing. Independently from this work, Dong et al. [25], recently mentioned the relation between OSDM and OTFS, however, without any mathematical proof or background. Therefore, in this paper, we show the mathematical equivalence of the two schemes, and show their relation to V-OFDM.

3. Modulation techniques

In this section, we discuss V-OFDM, OSDM and OTFS. By $\{s_k\}_{k=0}^{K-1}$ we denote the sequence of symbols we want to modulate and transmit over the channel. The output of the modulation will be denoted by $\{x_k\}_{k=0}^{K-1}$. To make a fair comparison, we will compare the modulation techniques without the source coding, transmit pulse and carrier frequency.

3.1. V-OFDM

V-OFDM divides the sequence of symbols into N subblocks of length M, thus $K = NM$. In matrix notation, $\mathbf{S} = [\mathbf{s}_0, \ldots, \mathbf{s}_{N-1}]$, where $\mathbf{s}_n = [s_{nM+0}, s_{nM+1} \ldots, s_{nM+M-1}]^T$. Then, an N-point IDFT is performed on the rows of $\mathbf{S}$. The modulated symbols become,[1]

$$\mathbf{x} = \text{vec}(\mathbf{S}\mathbf{F}_N^H) = \left((\mathbf{F}_N^H)^T \otimes \mathbf{I}_M\right)\text{vec}(\mathbf{S}) = (\mathbf{F}_N^H \otimes \mathbf{I}_M)\text{vec}(\mathbf{S}) = (\mathbf{F}_N^H \otimes \mathbf{I}_M)\mathbf{s}.$$
(1)

By performing an IDFT on the rows of $\mathbf{S}$ and vectorize columns of length M, it is as if we zero-pad each sample with $M - 1$ zeros before we compute the IDFT. As a result, we get M (block) repetitions in the frequency domain. Similarly we get repetitions in the time domain. The IDFT matrix $\mathbf{F}_N^H$ has N rows, so each element in $\mathbf{s}$ will appear N times in the output vector $\mathbf{x}$, resulting in N (block) repetitions in time. Fig. 1(c) shows the structure of the transmitted signal for V-OFDM.

From Fig. 1(c), one can see that if $(M \neq 1 \wedge N \neq 1)$, the structure of the transmitted signal of V-OFDM is fundamentally different from SCM, shown in Fig. 1(a), and OFDM, shown in Fig. 1(b). Each symbol now appears on an $M \times N$ grid.

From (1) it is clear that V-OFDM can make a compromise between SCM and OFDM. When $M = 1$, (1) reduces to $\mathbf{x} = \mathbf{F}_N^H\mathbf{s}$, and thus, V-OFDM is equal to OFDM. Similarly, when $N = 1$, (1) reduces to $\mathbf{x} = \mathbf{I}_M\mathbf{s}$, and V-OFDM equals SCM. Due to the flexibility, one would say that V-OFDM is generally more robust against Doppler spread than OFDM and more robust against intersymbol interference (ISI) than SCM. In Section 4 we will discuss its exact properties.

3.2. OSDM

Let $K = NM$. OSDM then splits the symbol sequence $\{s_k\}_{k=0}^{K-1}$ into N sequences of M symbols. Thus, again, $\mathbf{s}_n = [s_{nM+0}, s_{nM+1}, \ldots, s_{nM+M-1}]^T$ is the n'th sequence of M symbols, corresponding to the n'th column of $\mathbf{S}$. Then, the modulated $NM \times 1$ symbol vector $\mathbf{x}$ is the summation

---

[1] Note that for the matrices $\mathbf{A}$, $\mathbf{B}$ and $\mathbf{C}$, $\text{vec}(\mathbf{A}\mathbf{B}\mathbf{C}) = (\mathbf{C}^T \otimes \mathbf{A})\text{vec}(\mathbf{B})$, and that since $\mathbf{F}_N^H$ is square, $(\mathbf{F}_N^H)^T = \mathbf{F}_N^H$.

over all the columns, where to each column $\mathbf{s}_n$ the Kronecker product with $\mathbf{f}_n^*$, the $(n+1)$'th column of $\mathbf{F}_N^H$, is applied.

$$\mathbf{x} = \sum_{n=0}^{N-1} \mathbf{f}_n^* \otimes \mathbf{s}_n. \tag{2}$$

Note that, using the mixed-product property, the periodic cross-correlation between the sequences $(\mathbf{f}_{n_1}^* \otimes \mathbf{s}_{n_1})$ and $(\mathbf{f}_{n_2}^* \otimes \mathbf{s}_{n_2})$ is zero at every term for $n_1 \neq n_2$. The derivation of this property is given in Appendix. The zero periodic cross-correlation property is very useful as will become clear in Section 4.

However, (2) can be rewritten as follows,

$$\mathbf{x} = \sum_{n=0}^{N-1} \mathbf{f}_n^* \otimes \mathbf{s}_n = (\mathbf{F}_N^H \circ \mathbf{S})\mathbf{1}_{N \times 1} = \text{vec}(\mathbf{S}\mathbf{I}_N\mathbf{F}_N^H) \tag{3}$$
$$= \text{vec}(\mathbf{I}_M \mathbf{S}\mathbf{F}_N^H) = (\mathbf{F}_N^H \otimes \mathbf{I}_M)\text{vec}(\mathbf{S}) = (\mathbf{F}_N^H \otimes \mathbf{I}_M)\mathbf{s}.$$

From (3) it is clear that OSDM coincides with V-OFDM, as was remarked in [21,22]. The structure of the transmitted signal of OSDM can therefore also be depicted by Fig. 1(c). In [19] it was shown that OSDM (and thus also V-OFDM) has lower PAPR compared to OFDM.

We want to emphasize here that due to the mentioned zero periodic cross-correlation, the ISI (thus the interference between the block repetitions of $\mathbf{S}$ in Fig. 1(c)) is eliminated. Hence, V-OFDM and OSDM can do with only one CP per N repetitions of $\mathbf{S}$ in time [19].

3.3. OTFS

OTFS defines its symbols in the DD domain, $s_{\text{DD}}[k,l]$, for $k = 0, \ldots, M-1$ and $l = 0, \ldots, N-1$. The symbols are first mapped to the time–frequency (TF) domain using a combination of the inverse discrete symplectic Fourier transform (DSFT) and windowing [2], for $m = 0, \ldots, M-1$ and $n = 0, \ldots, N-1$,

$$s_{\text{TF}}[m,n] = w_{\text{tx}}[m,n]\frac{1}{\sqrt{NM}}\sum_{k=0}^{M-1}\sum_{l=0}^{N-1}s_{\text{DD}}[k,l]e^{-2\pi jm\frac{k}{M}}e^{2\pi jn\frac{l}{N}}, \tag{4}$$

where $w_{\text{tx}}[m,n]$ is the weight of the window. In literature, these weights are predominantly left out or set to one [13,26–29]. The use of weighting functions different from all ones was investigated in [30]. A performance improvement was found only when the estimated channel state information (CSI) is present at both the receiver and transmitter, which is a scenario that is never satisfied in practice. Additionally, the performance improvement is strongly dependent on the type of detection. Thus, choosing a different weighting function is in general not beneficial. Therefore, in this paper, we will use a weighting function of all ones.

Note that the DSFT is equivalent to consecutively performing an N-point IDFT and an M-point DFT on $s_{\text{DD}}[k,l]$. In matrix–vector notation one could write, $\mathbf{S}_{\text{TF}} = \mathbf{W}_{\text{tx}} \odot (\mathbf{F}_M\mathbf{S}_{\text{DD}}\mathbf{F}_N^H)$, where $\mathbf{S}_{\text{TF}}$, $\mathbf{W}_{\text{tx}}$ and $\mathbf{S}_{\text{DD}}$ are matrices of size $M \times N$ with elements $s_{\text{TF}}[m,n]$, $w_{\text{tx}}[m,n]$ and $s_{\text{DD}}[k,l]$, respectively. The symbols in the TF domain are then converted to the time domain by the Heisenberg transform [2],

$$x(t) = \sum_{m=0}^{M-1}\sum_{n=0}^{N-1}\frac{s_{\text{TF}}[m,n]}{\sqrt{M}}g_{\text{tx}}(t-nMT)e^{2\pi jm\frac{\Delta f}{M}(t-nMT)}, \tag{5}$$

where $g_{\text{tx}}(t)$ is the transmit pulse and $\Delta f = \frac{1}{T}$. From (5), one would not directly see the link between OTFS and V-OFDM and OSDM. However, by adopting the translation $t \to m'T + n'MT$ in (5) we can make the

connection. To do so, we write out the translation in (6),

$$x(m'T + n'MT) = \frac{1}{\sqrt{M}}\sum_{m=0}^{M-1}\sum_{n=0}^{N-1}s_{\text{TF}}[m,n]g_{\text{tx}}(m'T + n'MT$$
$$- nMT)e^{2\pi jm\frac{\Delta f}{M}(m'T+n'MT-nMT)}$$

$$\overset{(a)}{=} \frac{1}{\sqrt{M}}\sum_{m=0}^{M-1}s_{\text{TF}}[m,n']g_{\text{tx}}(m'T)e^{2\pi jm\frac{\Delta f}{M}(m'T)}$$

$$= g_{\text{tx}}(m'T)\frac{1}{\sqrt{M}}\sum_{m=0}^{M-1}s_{\text{TF}}[m,n']e^{2\pi jm\frac{m'}{M}}$$

$$= g_{\text{tx}}(m'T)\frac{1}{\sqrt{M}}\sum_{m=0}^{M-1}\left[w_{\text{tx}}[m,n']\frac{1}{\sqrt{NM}}\sum_{k=0}^{M-1}\sum_{l=0}^{N-1}s_{\text{DD}}[k,l]e^{-2\pi jm\frac{k}{M}}e^{2\pi j\frac{n'l}{N}}\right]$$
$$\times e^{2\pi jm\frac{m'}{M}}$$

$$\overset{(b)}{=} g_{\text{tx}}(m'T)\frac{1}{M\sqrt{N}}\sum_{m=0}^{M-1}\sum_{k=0}^{M-1}\sum_{l=0}^{N-1}s_{\text{DD}}[k,l]e^{-2\pi jm\frac{k-m'}{M}}e^{2\pi j\frac{n'l}{N}}$$

$$= g_{\text{tx}}(m'T)\frac{1}{\sqrt{N}}\sum_{l=0}^{N-1}\sum_{k=0}^{M-1}s_{\text{DD}}[k,l]\left[\frac{1}{M}\sum_{m=0}^{M-1}e^{-2\pi jm\frac{k-m'}{M}}\right]e^{2\pi j\frac{n'l}{N}}$$

$$\overset{(c)}{=} g_{\text{tx}}(m'T)\frac{1}{\sqrt{N}}\sum_{l=0}^{N-1}s_{\text{DD}}[m',l]e^{2\pi j\frac{n'l}{N}}. \tag{6}$$

where for (a) we have used that $g_{\text{tx}}(t)$ is zero outside the interval $[0, MT)$, for (b) we have used that $w_{\text{tx}}[m,n] = 1$ and for (c) we have used that,

$$\frac{1}{M}\sum_{m=0}^{M-1}e^{-2\pi jm\frac{k-m'}{M}} = \begin{cases} 1 & \text{if, } k = m' \\ 0 & \text{otherwise.} \end{cases} \tag{7}$$

Now we stack M samples of $x(t)$, namely $x(m'T + n'MT)$ for $m' = 0, 1, \ldots, M$, in one column. Using the result in (6) we can write,

$$\begin{bmatrix} x(0 \cdot T + n'MT) \\ x(1 \cdot T + n'MT) \\ \vdots \\ x((M-1)T + n'MT) \end{bmatrix}$$

$$= \frac{1}{\sqrt{N}}\sum_{l=0}^{N-1}e^{2\pi j\frac{n'l}{N}}\begin{bmatrix} g_{\text{tx}}(0 \cdot T) & \cdots & 0 \\ \vdots & \ddots & \vdots \\ 0 & \cdots & g_{\text{tx}}((M-1) \cdot T) \end{bmatrix}\begin{bmatrix} s_{\text{DD}}[0,l] \\ s_{\text{DD}}[1,l] \\ \vdots \\ s_{\text{DD}}[M-1,l] \end{bmatrix}$$

$$= \frac{1}{\sqrt{N}}\mathbf{G}_{\text{tx}}\begin{bmatrix} s_{\text{DD}}[0,0] & \cdots & s_{\text{DD}}[0,N-1] \\ \vdots & \ddots & \vdots \\ s_{\text{DD}}[M-1,0] & \cdots & s_{\text{DD}}[M-1,N-1] \end{bmatrix}\begin{bmatrix} 1 \\ e^{2\pi j\frac{n'}{N}} \\ \vdots \\ e^{2\pi j\frac{n'(N-1)}{N}} \end{bmatrix}$$

$$= \frac{1}{\sqrt{N}}\mathbf{G}_{\text{tx}}\mathbf{S}_{\text{DD}}\begin{bmatrix} 1 \\ e^{2\pi j\frac{n'}{N}} \\ \vdots \\ e^{2\pi j\frac{n'(N-1)}{N}} \end{bmatrix}. \tag{8}$$

Here $\mathbf{G}_{\text{tx}} = \text{diag}\left(g_{\text{tx}}(0 \cdot T), g_{\text{tx}}(1 \cdot T), \ldots, g_{\text{tx}}((M-1) \cdot T)\right)$ and $[\mathbf{S}_{\text{DD}}]_{m,n} = s_{\text{DD}}[m,n]$. If we then take N columns of M samples, we can write $\mathbf{X} = \mathbf{G}_{\text{tx}}\mathbf{S}_{\text{DD}}\mathbf{F}_N^H$, where $[\mathbf{X}]_{m,n} = x(mT + nMT)$. The modulated symbols including a transmit pulse are,

$$\mathbf{x} = \text{vec}(\mathbf{X}) = \text{vec}(\mathbf{G}_{\text{tx}}\mathbf{S}_{\text{DD}}\mathbf{F}_N^H) = (\mathbf{F}_N^H \otimes \mathbf{G}_{\text{tx}})\mathbf{s} = (\mathbf{I}_N \otimes \mathbf{G}_{\text{tx}})(\mathbf{F}_N^H \otimes \mathbf{I}_M)\mathbf{s}. \tag{9}$$

where $\mathbf{s} = \text{vec}(\mathbf{S}_{\text{DD}})$. Note that, by not considering the transmit pulse for V-OFDM and OTFS, it is implicitly assumed that a rectangular (transmit) pulse is used. Therefore, to make a fair comparison with the other modulation schemes, we should use a rectangular pulse for OTFS as well, such that the transmitted symbols for OTFS become

$$\mathbf{x} = (\mathbf{F}_N^H \otimes \mathbf{I}_M)\mathbf{s}. \tag{10}$$

From (10) it is clear that OTFS coincides with V-OFDM and OSDM.

Before we continue, a final remark about the transmit pulse is in order. In [2] it is assumed that the transmit and receive pulses $g_{tx}(t)$ and $g_{rx}(t)$ are bi-orthogonal with respect to a translation of an integer multiple of MT in time and $1/MT$ in frequency. Additionally, it is assumed that $g_{tx}(t)$ and $g_{rx}(t)$ are bi-orthogonal with respect to a translation of an integer multiple of T in time, within the support of the channel (maximum time delay), and to a translation of an integer multiple of $1/T$ in frequency, within the support of the channel (maximum frequency shift). This can actually never be satisfied by $g_{tx}(t)$ and $g_{rx}(t)$ in practice [28]. In current literature a rectangular pulse is predominantly used (see e.g. [13,27,28]), since the use of a rectangular function for the transmit pulse is the optimal in terms of BER (see [29], Fig. 1).

4. Influence of the channel

In this section, we will discuss the properties of V-OFDM/OSDM/ OTFS with respect to different channel characteristics. We want to stress, however, that the equivalence between the modulation schemes, as shown in the previous section, does not depend on these channel characteristics.

In Section 3.2 we saw that for V-OFDM/OSDM/OTFS, the modulated symbol vector $\mathbf{x}$ is the summation over the sequences $(\mathbf{f}_n^* \otimes \mathbf{s}_n)$, which have zero periodic-cross correlation across n. In this section, we investigate if this property remains after propagating through the channel with delay and Doppler spread.

The communication channel can be approximated by a basis expansion model (BEM) [31,32]. In a BEM, the delays[2] are modeled by a linear filter, which (assuming a CP is used) is described by a circulant matrix $\mathbf{H}_q \in \mathbb{C}^{K \times K}$, defined by the taps of the filter, $h_{k,q}$ for $k = 0, 1, \ldots, K - 1$. A Doppler shift is modeled by a diagonal matrix, $\boldsymbol{\Lambda}_q = \mathrm{diag}(W_K^0, W_K^q, \ldots, W_K^{(K-1)q})$. An effective channel with both delays and Doppler shifts is thus described by, $\mathbf{H}_{\mathrm{eff}} = \sum_{q=-Q}^{Q} \boldsymbol{\Lambda}_q \mathbf{H}_q$.

Let $\mathbf{P}_K$ be the cyclic permutation matrix of size K. As was mentioned earlier (and shown in Appendix), the sequences have zero periodic-cross correlation across n, that is,

$$(\mathbf{f}_{n_1}^* \otimes \mathbf{s}_{n_1})^H \mathbf{P}_K^k (\mathbf{f}_{n_2}^* \otimes \mathbf{s}_{n_2}) = 0, \quad n_1 \neq n_2, \ \forall k \in \{0, 1, \ldots K - 1\}. \tag{11}$$

We note that a circulant matrix is a summation of weighted cyclic permutation matrices, i.e. $\mathbf{H}_q = \sum_{k=0}^{K-1} h_{k,q} \mathbf{P}_K^k$. As a result, the sequences remain orthogonal after propagating through a channel $\mathbf{H}_q$ without Doppler shifts with only (possibly multiple) delays,

$$\begin{aligned}
(\mathbf{f}_{n_1}^* \otimes \mathbf{s}_{n_1})^H \mathbf{H}_q (\mathbf{f}_{n_2}^* \otimes \mathbf{s}_{n_2}) &= (\mathbf{f}_{n_1}^* \otimes \mathbf{s}_{n_1})^H \Big(\sum_{k=0}^{K-1} h_{k,q} \mathbf{P}_K^k \Big) (\mathbf{f}_{n_2}^* \otimes \mathbf{s}_{n_2}) \\
&= \sum_{k=0}^{K-1} h_{k,q} (\mathbf{f}_{n_1}^* \otimes \mathbf{s}_{n_1})^H \mathbf{P}_K^k (\mathbf{f}_{n_2}^* \otimes \mathbf{s}_{n_2}) \\
&= \sum_{k=0}^{K-1} h_{k,q} \cdot 0 = 0, \quad n_1 \neq n_2.
\end{aligned} \tag{12}$$

This means that there is no ISI between the symbols of different sequences and as such the receiver can process the sequences independently. This can be further clarified when we look at the transfer function between transmitter and receiver where the modulation, the channel and the demodulation are aggregated. The receiver demodulates the received signal using $(\mathbf{F}_N \otimes \mathbf{I}_M)$. The transfer function for the symbols becomes,

$$\bar{\mathbf{H}}_1 = (\mathbf{F}_N \otimes \mathbf{I}_M) \mathbf{H}_q (\mathbf{F}_N^H \otimes \mathbf{I}_M). \tag{13}$$

The matrix $\bar{\mathbf{H}}_1$ is block diagonal (N blocks of size M) [33], due to the zero cross-correlation property in (12).

However, the sequences do not remain orthogonal if a delay and Doppler shift is considered, since $\boldsymbol{\Lambda}_q \mathbf{H}_q$ is not circulant and thus not a summation of weighted permutation matrices anymore. There exists at least one pair[3] $(n_1, n_2) \in \{1, 2 \ldots, N\}^2$ such that $n_1 \neq n_2$, for which,

$$(\mathbf{f}_{n_1}^* \otimes \mathbf{s}_{n_1})^H \boldsymbol{\Lambda}_q \mathbf{H}_q (\mathbf{f}_{n_2}^* \otimes \mathbf{s}_{n_2}) \neq 0. \tag{14}$$

Therefore, the receiver cannot process the sequences independently anymore. Moreover, since the sequences do not remain orthogonal, the transfer function,

$$\bar{\mathbf{H}}_2 = (\mathbf{F}_N \otimes \mathbf{I}_M) \boldsymbol{\Lambda}_q \mathbf{H}_q (\mathbf{F}_N^H \otimes \mathbf{I}_M), \tag{15}$$

is not block diagonal, which is another way of describing that the sequences cannot be processed independently.

Overall, we can conclude the following about the tolerance of V-OFDM/OSDM/OTFS against Doppler shifts. If the channel experiences only one Doppler shift, thus a channel of the form $\boldsymbol{\Lambda}_{q_1} \mathbf{H}_{q_1}$, the receiver can still compensate for this one Doppler shift *before* demodulation and further processing, namely by multiplying with $\boldsymbol{\Lambda}_{q_1}^{-1}$. Hence, interference between sequences can still be avoided. However, when the communication channel consists of multiple delays, of which at least two have different Doppler shifts, thus a channel of the form $\sum_i \boldsymbol{\Lambda}_{q_i} \mathbf{H}_{q_i}$, this compensation before demodulation is not possible anymore. Consequently, interference between different sequences is inevitable.

Therefore, the claim that V-OFDM/OSDM/OTFS is more robust against Doppler shifts than OFDM (e.g. [2]) should be interpreted carefully. V-OFDM/OSDM/OTFS can only outperform OFDM if the right processing is performed at the receiver. Han et al. [33] described such a receiver that cancels the ICI between the blocks in $\bar{\mathbf{H}}_2$. Alternatively, Raviteja et al. [29] describe a receiver in the delay-Doppler domain. Similar to OFDM, V-OFDM/OSDM/OTFS can also have guard bands to be (more) tolerant of large Doppler spread, as was proposed in [34] and was called Doppler resilient OSDM (D-OSDM).

5. Conclusion

In this paper, we have shown that OSDM and OTFS are mathematically equivalent by deriving the input–output relation of the modulation techniques from the first principles presented in [1,2], respectively. Additionally, we have given insight in the performance in terms of ISI and ICI by discussing its signal structure.

Due to the equivalence, all the results that have been presented in underwater communications on OSDM can be carried over and continued in RF communications on OTFS, and vice versa. We conclude that, while OTFS may be derived from different principles, the resulting modulation technique is equivalent to V-OFDM, A-OFDM (shown in [13,23]) and OSDM (shown in this paper) which where all invented prior to OTFS.

CRediT authorship contribution statement

Ids van der Werf: Conceptualization, Formal analysis, Visualization, Writing – original draft. **Henry Dol:** Supervision, Writing – review & editing. **Koen Blom:** Supervision, Writing – review & editing. **Richard Heusdens:** Supervison, Writing – review & editing. **Richard C. Hendriks:** Supervision, Writing – review & editing. **Geert Leus:** Conceptualization, Formal analysis, Writing – review & editing.

Declaration of competing interest

The authors declare the following financial interests/personal relationships which may be considered as potential competing interests: Co-author Geert Leus is editor-in-chief of the Elsevier SP journal.

---

[2] Note that delay spread and Doppler spread encompasses the collective effect of all the delays and Doppler shifts respectively. Hence, the effect of delay spread and Doppler spread are discussed in terms of multiple delays and Doppler shifts.

---

[3] For example, all pairs that satisfy $q = n_1 - n_2 \neq 0$.

Data availability

No data was used for the research described in the article.

Appendix. Orthogonality of sequences of V-OFDM/OSDM/OTFS

In this appendix we will show that the sequences that of the OSDM signal have zero periodic cross-correlation. Let the sequences be defined by $(\mathbf{f}_n^* \otimes \mathbf{s}_n)$, and let $\mathbf{P}_K$ be a cyclic permutation matrix of size $K = NM$.

First, note that the columns of a (I)DFT matrix are orthogonal, $\mathbf{f}_{n_1}^{*\,H}\mathbf{f}_{n_2}^* = 0$, if $n_1 \neq n_2$, and remain orthogonal also after a cyclic permutation, thus we have,

$$\mathbf{f}_{n_1}^{*\,H}\mathbf{P}_N^k\mathbf{f}_{n_2}^* = 0, \quad n_1 \neq n_2, \forall k \in \{0,1,\dots,K-1\}. \tag{16}$$

Then, note that the sequences are orthogonal, that is,

$$(\mathbf{f}_{n_1}^* \otimes \mathbf{s}_{n_1})^H(\mathbf{f}_{n_2}^* \otimes \mathbf{s}_{n_2}) = (\mathbf{f}_{n_1}^{*\,H}\mathbf{f}_{n_2}^*)\otimes(\mathbf{s}_{n_1}^{\,H}\mathbf{s}_{n_2}) = 0\otimes(\mathbf{s}_{n_1}^{\,H}\mathbf{s}_{n_2}) = 0, \quad n_1 \neq n_2. \tag{17}$$

We can rewrite the cyclic permutation matrix, $\mathbf{P}_K = \mathbf{I}_N \otimes \mathbf{L}_M + \mathbf{P}_N \otimes \mathbf{U}_M$, where $\mathbf{L}_M$ is a cyclic permutation matrix of size M except for the top right element, which is zero, and $\mathbf{U}_M$ is a zero matrix of size M except for the top right element, which is one (thus $\mathbf{P}_M = \mathbf{L}_M + \mathbf{U}_M$). For the sequences we can then show that,

$$\begin{aligned}
&(\mathbf{f}_{n_1}^* \otimes \mathbf{s}_{n_1})^H\mathbf{P}_K(\mathbf{f}_{n_2}^* \otimes \mathbf{s}_{n_2})\\
&= (\mathbf{f}_{n_1}^* \otimes \mathbf{s}_{n_1})^H(\mathbf{I}_N \otimes \mathbf{L}_M + \mathbf{P}_N \otimes \mathbf{U}_M)(\mathbf{f}_{n_2}^* \otimes \mathbf{s}_{n_2}) =\\
&= \left(\mathbf{f}_{n_1}^{*\,H}(\mathbf{I}_N + \mathbf{P}_N)\mathbf{f}_{n_2}^*\right) \otimes \left(\mathbf{s}_{n_1}^{\,H}(\mathbf{L}_M + \mathbf{U}_M)\mathbf{s}_{n_2}\right)\\
&= (0+0)\otimes\left(\mathbf{s}_{n_1}^{\,H}(\mathbf{L}_M + \mathbf{U}_M)\mathbf{s}_{n_2}\right) = 0 \quad n_1 \neq n_2.
\end{aligned} \tag{18}$$

Thus the sequences remain orthogonal after a cyclic permutation. To show that the sequences of OSDM have zero periodic cross-correlation, we have to show their orthogonality for (all) multiple cyclic permutations. For two cyclic permutations we can write,

$$\begin{aligned}
\mathbf{P}_K^2 &= (\mathbf{I}_N \otimes \mathbf{L}_M + \mathbf{P}_N \otimes \mathbf{U}_M)^2\\
&= (\mathbf{I}_N^2 \otimes \mathbf{L}_M^2) + (\mathbf{P}_N^2 \otimes \mathbf{U}_M^2) + (\mathbf{P}_N \otimes \mathbf{L}_M\mathbf{U}_M) + (\mathbf{P}_N \otimes \mathbf{U}_M\mathbf{L}_M).
\end{aligned} \tag{19}$$

Note that for any number of cyclic permutations, one can always write

$$\mathbf{P}_K^k = \sum_{i=1}^{2^k} f_i(\mathbf{I}_N,\mathbf{P}_N) \otimes g_i(\mathbf{L}_M,\mathbf{U}_M), \quad k \in \{0,1,\dots,K-1\}, \tag{20}$$

where $f_i(\mathbf{I}_N,\mathbf{P}_N)$ is a function which depends only on $\mathbf{I}_N$ and $\mathbf{P}_N$, and $g_i(\mathbf{L}_M,\mathbf{U}_M)$ is a function which depends only on $\mathbf{L}_M$ and $\mathbf{U}_M$. Now we can show that the sequences of OSDM have zero periodic cross-correlation,

$$\begin{aligned}
&(\mathbf{f}_{n_1}^* \otimes \mathbf{s}_{n_1})^H\mathbf{P}_K^k(\mathbf{f}_{n_2}^* \otimes \mathbf{s}_{n_2})\\
&= (\mathbf{f}_{n_1}^* \otimes \mathbf{s}_{n_1})^H(\mathbf{I}_N \otimes \mathbf{L}_M + \mathbf{P}_N \otimes \mathbf{U}_M)^k(\mathbf{f}_{n_2}^* \otimes \mathbf{s}_{n_2})\\
&= (\mathbf{f}_{n_1}^* \otimes \mathbf{s}_{n_1})^H\left[\sum_{i=1}^{2^k} f_i(\mathbf{I}_N,\mathbf{P}_N) \otimes g_i(\mathbf{L}_M,\mathbf{U}_M)\right](\mathbf{f}_{n_2}^* \otimes \mathbf{s}_{n_2})\\
&= \left(\mathbf{f}_{n_1}^{*\,H}\left[\sum_{i=1}^{2^k} f_i(\mathbf{I}_N,\mathbf{P}_N)\right]\mathbf{f}_{n_2}^*\right) \otimes \left(\mathbf{s}_{n_1}^{\,H}\left[\sum_{i=1}^{2^k} g_i(\mathbf{L}_M,\mathbf{U}_M)\right]\mathbf{s}_{n_2}\right)\\
&= 0 \otimes \left(\mathbf{s}_{n_1}^{\,H}\left[\sum_{i=1}^{2^k} g_i(\mathbf{L}_M,\mathbf{U}_M)\right]\mathbf{s}_{n_2}\right) = 0 \quad n_1 \neq n_2, \forall k \in \{0,1\dots,K-1\}.
\end{aligned} \tag{21}$$

References

[1] N. Suehiro, C. Han, T. Imoto, N. Kuroyanagi, An information transmission method using Kronecker product, in: Proc. IASTED Int. Conf. Commun. Syst. Netw., 2002, pp. 206–209.

[2] R. Hadani, et al., Orthogonal time frequency space modulation, in: 2017 IEEE Wireless Commun. Netw. Conf., WCNC, 2017, pp. 1–6.

[3] T. Wang, J.G. Proakis, E. Masry, J.R. Zeidler, Performance degradation of OFDM systems due to Doppler spreading, IEEE Trans. Wireless Commun. 5 (6) (2006) 1422–1432.

[4] R. Hadani, et al., Orthogonal time frequency space modulation, 2022, [Online]. Available: https://arxiv.org/pdf/1808.00519.pdf. (Accessed on: 05 October 2022).

[5] 3GPP R1- 1610397, OTFS PAPR analysis, Cohere Technologies.

[6] B. Xu, Z. Xia, R. Liu, Y. Zhang, J. Hu, W. Xie, Research on OTFS modulation applied in LTE-based 5G terrestrial broadcast, in: 2020 Int. Wireless Commun. Mobile Comput., IWCMC, 2020, pp. 514–519.

[7] A. Gunturu, A.R. Godala, A.K. Sahoo, A.K.R. Chavva, Performance analysis of OTFS waveform for 5G NR mmwave communication system, in: 2021 IEEE Wireless Commun. Netw. Conf., WCNC, 2021, pp. 1–6.

[8] S.S. Das, R. Prasad, OTFS: Orthogonal Time Frequency Space Modulation a Waveform for 6G, River Publishers, 2021, pp. i–xxvi.

[9] R. Hadani, S. Rakib, OTFS methods of data channel characterization and uses thereof, 2016, U.S. Patent 9 444 541 B2.

[10] G. Fettweis, M. Krondorf, S. Bittner, GFDM - generalized frequency division multiplexing, in: VTC Spring 2009 - IEEE 69th Veh. Technol. Conf., 2009, pp. 1–4.

[11] A. Nimr, M. Chafii, M. Matthe, G. Fettweis, Extended GFDM framework: OTFS and GFDM comparison, in: 2018 IEEE Global Commun. Conf., GLOBECOM, 2018, pp. 1–6.

[12] J. Zhang, A.D.S. Jayalath, Y. Chen, Asymmetric OFDM systems based on layered FFT structure, IEEE Signal Process. Lett. 14 (11) (2007) 812–815.

[13] P. Raviteja, E. Viterbo, Y. Hong, OTFS performance on static multipath channels, IEEE Wirel. Commun. Lett. 8 (3) (2019) 745–748.

[14] M. Stojanovic, J. Catipovic, J. Proakis, Phase coherent digital communications for underwater acoustic channels, IEEE J. Ocean. Eng. 19 (1) (1994) 100–111.

[15] S. Coatelan, A. Glavieux, Design and test of a coding OFDM system on the shallow water acoustic channel, in: Proc. OCEANS Conf., Vol. 3, 1995, pp. 2065–2070.

[16] N. Suehiro, Chenggao. Han, T. Imoto, Very efficient wireless frequency usage based on pseudo-coherent addition of multipath signals using Kronecker product with rows of DFT matrix, in: IEEE Int. Symp. Inform. Theory, 2003. Proc., 2003, pp. 385–385.

[17] N. Suehiro, R. Jin, C. Han, T. Hashimoto, Performance of very efficient wireless frequency usage system using Kronecker product with rows of DFT matrix, in: 2006 IEEE Inform. Theory Workshop - ITW '06 Chengdu, 2006, pp. 526–529.

[18] T. Ebihara, N. Suehiro, The orthogonal signal division multiplexing and its performance evaluation (in Japanese), IEICE Trans. J91-B (2008) 1086–1094.

[19] T. Ebihara, K. Mizutani, Underwater acoustic communication with an orthogonal signal division multiplexing scheme in doubly spread channels, IEEE J. Ocean Eng. 39 (1) (2014) 47–58.

[20] X.-G. Xia, Precoded and vector OFDM robust to channel spectral nulls and with reduced cyclic prefix length in single transmit antenna systems, IEEE Trans. Commun. 49 (8) (2001) 1363–1374.

[21] C. Han, T. Hashimoto, N. Suehiro, Constellation-rotated vector OFDM and its performance analysis over Rayleigh fading channels, IEEE Trans. Commun. 58 (3) (2010) 828–838.

[22] T. Ebihara, H. Ogasawara, Underwater acoustic communication using Doppler-resilient orthogonal signal division multiplexing with time diversity, in: OCEANS 2017 - Aberdeen, 2017, pp. 1–9.

[23] P. Cheng, M. Tao, Y. Xiao, W. Zhang, V-OFDM: On performance limits over multi-path Rayleigh fading channels, IEEE Trans. Commun. 59 (7) (2011) 1878–1892.

[24] X.-G. Xia, Comments on the transmitted signals of OTFS and VOFDM are the same, IEEE Trans. Wirel. Commun. 21 (12) (2022) 11252.

[25] Y. Dong, J. Lei, Y. Huang, K. Lai, A look at OTFS from a hybrid carrier perspective, in: 2022 10th Int. Workshop Signal Des. Applicat. Commun., IWSDA, 2022, pp. 1–5.

[26] M.N. Hossain, Y. Sugiura, T. Shimamura, H.-G. Ryu, Waveform design of low complexity WR-OTFS system for the OOB power reduction, in: 2020 IEEE Wireless Commun. Netw. Conf. Workshops, WCNCW, 2020, pp. 1–5.

[27] L. Xiao, S. Li, Y. Qian, D. Chen, T. Jiang, An overview of OTFS for Internet of Things: Concepts, benefits, and challenges, IEEE Internet Things J. 9 (10) (2022) 7596–7618.

[28] P. Raviteja, K.T. Phan, Y. Hong, E. Viterbo, Interference cancellation and iterative detection for orthogonal time frequency space modulation, IEEE Trans. Wirel. Commun. 17 (10) (2018) 6501–6515.

[29] P. Raviteja, Y. Hong, E. Viterbo, E. Biglieri, Practical pulse-shaping waveforms for reduced-cyclic-prefix OTFS, IEEE Trans. Veh. Technol. 68 (1) (2019) 957–961.

[30] Z. Wei, W. Yuan, S. Li, J. Yuan, D.W.K. Ng, Transmitter and receiver window designs for orthogonal time-frequency space modulation, IEEE Trans. Commun. 69 (4) (2021) 2207–2223.

[31] M.K. Tsatsanis, G.B. Giannakis, Modelling and equalization of rapidly fading channels, Int. J. Adaptive Control Signal Process. 10 (1996) 159–176.

[32] G.B. Giannakis, C. Tepedelenlioglu, Basis expansion models and diversity techniques for blind identification and equalization of time-varying channels, Proc. IEEE 86 (10) (1998) 1969–1986.

[33] J. Han, S.P. Chepuri, Q. Zhang, G. Leus, Iterative per-vector equalization for orthogonal signal-division multiplexing over time-varying underwater acoustic channels, IEEE J. Ocean. Eng. 44 (1) (2019) 240–255.

[34] T. Ebihara, G. Leus, Doppler-resilient orthogonal signal-division multiplexing for underwater acoustic communication, IEEE J. Ocean. Eng. 41 (2) (2016) 408–427.